CoolCAT

Thomas R. Ayres[1]

Center for Astrophysics & Space Astronomy, 389 UCB, University of Colorado, Boulder, CO 80309, USA

Abstract

http://casa.colorado.edu/~ayres/CoolCAT is a digital catalog of *HST* STIS echelle spectra of late-type stars, uniformly processed, coadded, and concatenated; the equivalent of an ultraviolet spectral atlas for each of about 50 objects.

Key words: Stars: late-type – Spectra: ultraviolet – Instruments: HST/STIS

1. Introduction

With support from the *HST* archival program, I constructed an extensive catalog of UV spectra of late-type stars based on echelle mode exposures taken by the Space Telescope Imaging Spectrograph (STIS: Woodgate et al. 1998) over the period 1997–2003. The objective was to collect together the disparate STIS observations of cool stars by many different observers, process the echellograms uniformly, combine exposures taken in the same grating mode consistently, and concatenate different wavelength regions into a single spectral trace for each object. The motivation was to develop full coverage UV "atlases" of a diverse set of cool stars to enable a wide variety of investigations that benefit from comparative studies of a particular spectral diagnostic in many stars, many diagnostics in a single star, or both. A recent example is a search for coronal forbidden lines in UV spectra of late-type stars (Ayres et al. 2003).

The 1150–3000 Å ultraviolet region[1] is an old friend to astronomers who study physical processes connected with magnetic activity in the outer atmospheres of late-type stars. The UV contains important emission (and sometimes absorption) features that form in chromospheres ($T \sim 10^4$ K: e.g., H I λ1215 Lyα, Mg II $\lambda\lambda$2795,2802), transition zones ($T \sim 10^5$ K: e.g., C IV $\lambda\lambda$1548,50), and even coronal plasmas ($T > 10^6$ K: Fe XII λ1242, Fe XXI λ1354). High spectral resolution measurements not only can separate key diagnostics from contaminating blends, but also record the line shapes, which carry vital clues to the dynamical state of the gas through Doppler shifts, nonthermal broadening, and discrete absorption components due to outflows (or accretion in the case of very young stars).

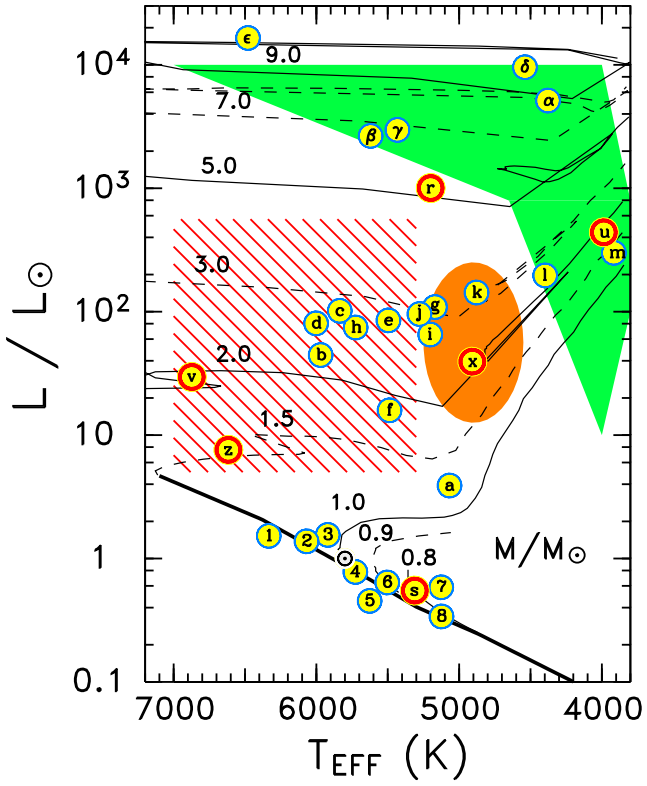

Figure 1. Prominent members of CoolCAT in H–R diagram.

2. Space Telescope Imaging Spectrograph

STIS is[2] a high-performance multi-mode spectrometer with two of the best microchannel-plate intensified UV cameras (1K×1K MAMAs) ever built for flight. (STIS also has a CCD camera with some UV response, but it is rarely used shortward of 3000 Å.) The far-UV MAMA utilizes a "solar-blind" photocathode, which is extremely valuable for observations of faint but diagnostically important

[1] Delimited at the shortward end by the magnesium-fluoride windows commonly used in space-qualified UV cameras.

[2] Or, I should say "was," since as of this writing the Solar System's premier ultraviolet spectrograph has run out of 5-Volt power supplies, and is—barring a miracle—effectively dead.

emission features in the $\lambda < 1700$ Å region, without the distracting influence of background light scattered from the intense photospheric glare longward of 2000 Å.

STIS has an impressive number of different mode combinations — apertures, filters, and grating choices — although only a relative handful have been characterized fully. One of the beauties of STIS is that the whole UV interval 1150–3000 Å can be covered with only about four overlapping echelle grating settings, and the especially important region shortward of 1700 Å can be captured in a single shot (E140M mode). This means, first of all, that most observers use a standard sequence of grating settings, which makes the STIS archive highly homogeneous and uniform. Secondly, the dominantly photospheric absorption spectrum longward of 1700 Å is so bright that obtaining a high-S/N recording of the full interval usually requires only a fraction of the exposure time needed to reach the faint dominantly emission spectrum shortward. This encourages observers to obtain an entire UV spectrum of their target even when the main interest is in the chromospheric emission line spectrum down near Lyα. Thirdly, although investigations like those involving the interstellar medium (e.g., Redfield, Wood, & Linsky 2004) or astrospheric "hydrogen walls" (Wood 2004) regard their late-type targets merely as background light sources, the wavelength coverage even in the highest resolution echelle modes is so broad that a big chunk of useful chromospheric spectral territory comes along for the ride in exposures aimed at one or a few ISM metal absorptions or Lyα itself. The reverse is true, as well: STIS programs probing chromospheric emission-line stars often produce material that is valuable, say, to ISM investigators.

CoolCAT focussed solely on the echelle modes, because of their broad systematic spectral coverage, and high spectral resolution ($R \equiv \lambda/\Delta\lambda$ of 3–4$\times10^4$ in the medium-resolution ["M"] modes; and 1.1$\times10^5$ in the high-resolution ["H"] modes). Observing programs that utilized the first-order dispersers on STIS, often taking advantage of the long-slit imaging capability, are less valuable for a cataloging effort because the wavelength coverage is sporadic (only about 50 Å per shot in the far-UV) and resolution ($\sim 10^4$) much lower than the echelle modes.

3. The Cool Star Sample

The catalog includes those cool stars in the *HST* archive as of March 2003 having publicly available STIS data taken in one or more of the echelle modes. Candidate objects were identified using a variety of strategies with the search engine of the Multi-mission Archive at Space Telescope (MAST, which will be the ultimate repository of CoolCAT itself). Unusual objects like cataclysmic variables, symbiotics, and eclipsing binaries of the Zeta Aurigae class were avoided; although T-Tauri stars were included. A total of 52 objects inhabit the catalog as of 2004 August, ten of which are T Tauris. A more detailed breakdown follows

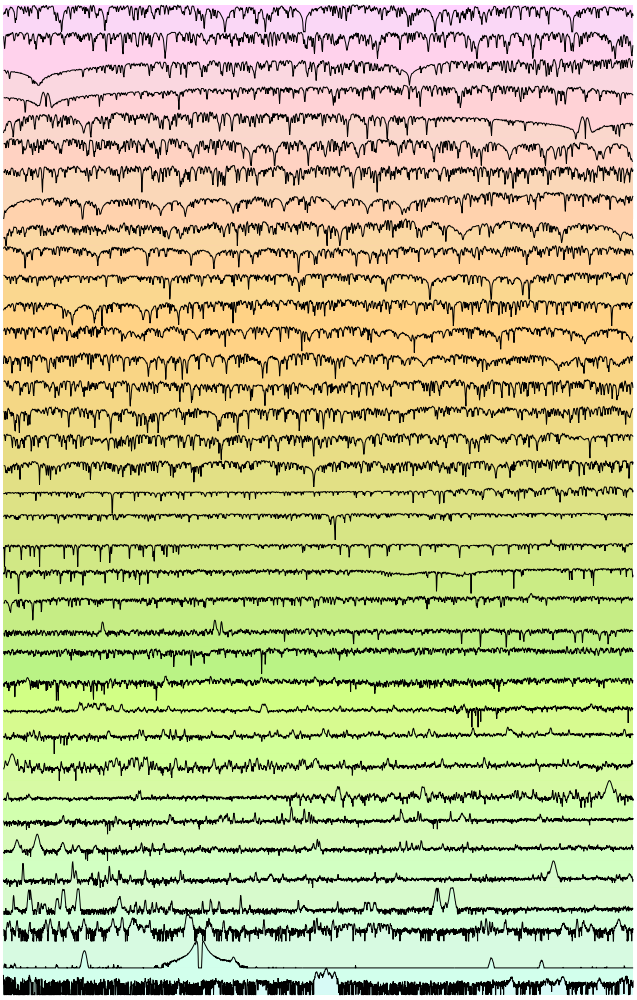

Figure 2. Full spectrum 1150–3000 Å of solar twin α Cen A.

(values in parentheses are the number of stars with complete spectral coverage 1150–3000 Å): four (4) G–K supergiants ; twelve (6) F–K giants; twenty-six (7) F–M dwarfs (including four dMe flare stars); and ten (5) T Tauris (the quality of the latter, in general, is poorer than the other stars). All of the targets, except for Procyon (αCMi: F5 IV-V), have at least one exposure in the far-UV region ($\lambda < 1700$ Å); although eighteen of the stars have no echelle coverage longward of 1700 Å.

Figure 1 depicts an H–R diagram of some of the prominent catalog targets, marked as thin (blue) outlined circles. The thicker (red) outlined symbols refer to important stars that were observed early in the *HST* mission by the Goddard High-Resolution Spectrograph (GHRS), but unfortunately not subsequently with second-generation STIS. The spotty wavelength coverage of GHRS renders these targets unsuitable for CoolCAT. The hatched (red) region is the Hertzsprung gap; the shaded (orange) oval is the core-helium burning "clump," and the shaded polygonal (green) area outlines the zone where cool stellar winds are common (and hot coronae are less conspicuous).

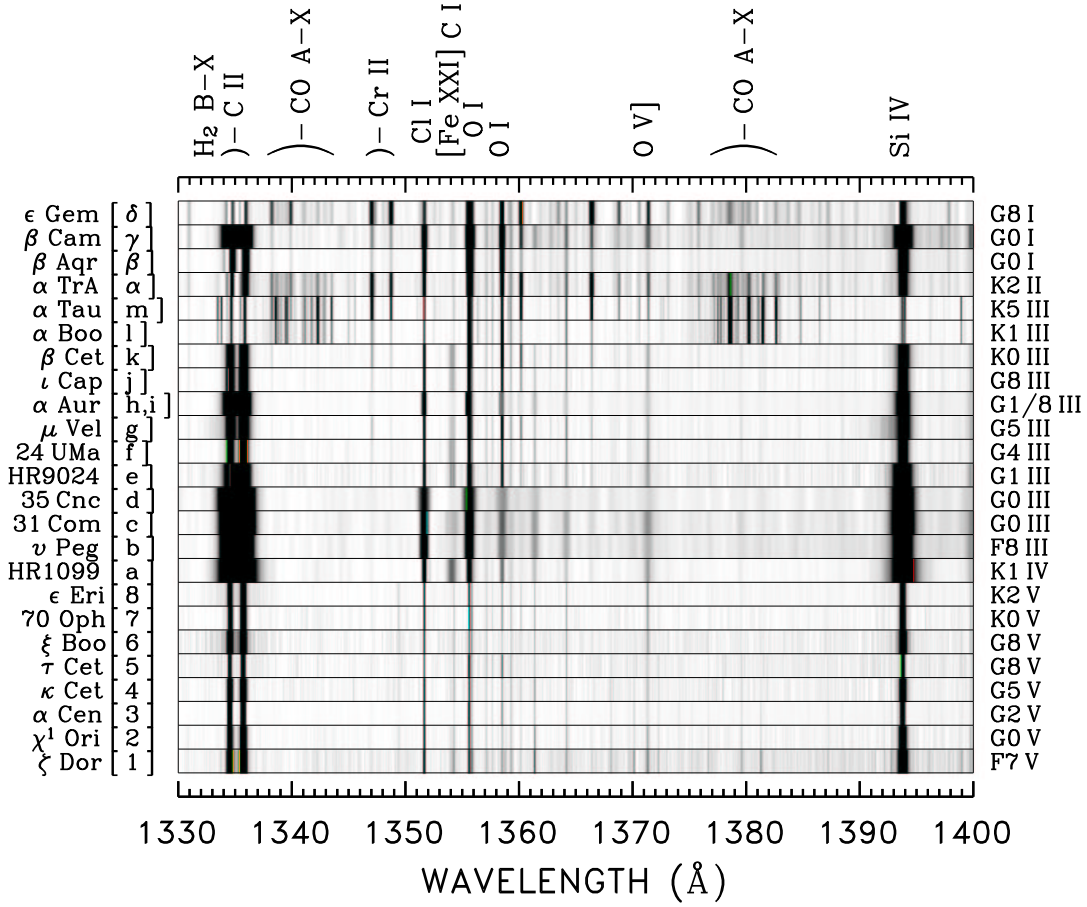

Figure 3. 1330–1400 Å spectral region in objects of Fig. 1.

4. Spectral Reductions

For each echelle observation, the individual echelle orders from the standard pipeline processing (including the new scattered light correction) were spliced together to form a continuous 1-D spectrum. If more than one observation was available in a given echelle mode setting, these were coadded using cross-correlation to align the exposures to a common wavelength scale. If two or more different mode settings were available, the segments were concatenated. The flux scales of the segments were adjusted, if necessary, to match calibrated *IUE* spectral energy distributions (as available). A detailed description of the CoolCAT procedures and rationales can be found in a forthcoming journal article (to be submitted to PASP).

Figure 2 depicts the CoolCAT spectrum of the solar twin α Cen A (see, also, Pagano et al. 2004). Each slice is 50 Å long, starting from 1150 Å at the bottom, extending to 3000 Å at the top; the flux scale is logarithmic. This is the best example from the catalog, because the observers used exclusively the high-resolution ($R \sim 110{,}000$) echelle modes and took care to expose each segment deeply enough to bring up the fainter spectral structure. In fact, the α Cen UV spectrum is much better, in terms of resolution and S/N, than the best available for the *Sun.*

Figure 3 compares CoolCAT spectra in the region 1330–1400 Å of objects marked in Fig. 1. The wide range of diagnostic species present is impressive: from molecules like CO and H_2 ($T \sim 2000$ K), to strong chromospheric lines of C II (2×10^4 K), transition zone emissions of Si IV (6×10^4 K) and semi-permitted O V (2×10^5 K), all the way up to coronal forbidden line Fe XXI (1×10^7 K). The fast spinning Hertzsprung gap giants (F8–G0 III) display prominent rotational broadening, while the archetype "noncoronal" red giants α Boo and α Tau show blueshifted wind absorptions in C II plus an array of fluoresced molecular bands.

5. Application: Transition Zone Dynamics

Many applications can be envisioned for CoolCAT. I will mention one here, namely the dynamics of stellar transition zones revealed by multicomponent Gaussian deconvolutions of UV line profiles. Wood, Linsky, & Ayres (1997) demonstrated that GHRS profiles of UV transition zone lines like Si IV and C IV, which form near 10^5 K, could be decomposed into "narrow" and "broad" components. The authors speculated that the broad components, in particular, which are always highly supersonic, could represent the stellar equivalent of solar "transition zone explosive events," and thereby account for a significant fraction of the subcoronal heating, in localized violent releases of magnetic energy.

STIS spectra have significant advantages over the first generation GHRS observations for addressing issues connected with the dynamical lineshapes of the UV "hot lines." First, with STIS's E140M mode, the entire 1150–1700 Å interval is recorded in a single exposure, thus ensuring not only a rich selection of diagnostic lines, but also that each one has experienced the same temporal environment as all the others. With sequential GHRS exposures of narrow wavelength regions, the Si IV lines might have been captured during a quiescent period, say, while C IV might have been caught during a flaring interval. Secondly, STIS has a very secure wavelength calibration, each new grating movement is accompanied by a lamp spectrum to calibrate the zero-point wavelength shift, and accurate peak-ups into the narrow STIS apertures ensure well centered target images. Finally, the STIS E140M resolution is about twice that of the corresponding GHRS first-order grating modes, which is important when measuring lineshapes of relatively narrow chromospheric features, as well as generally reducing the influence of the line spread function on all the UV emission line profiles.

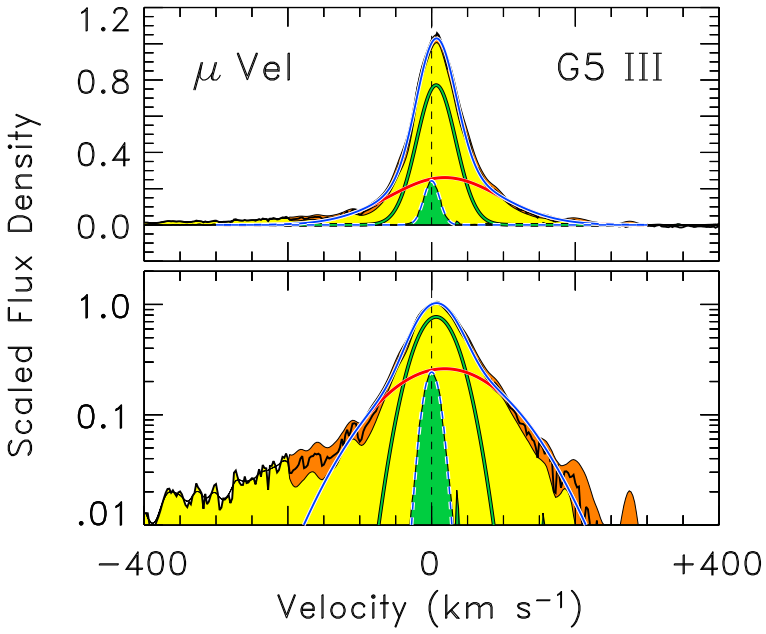

Figure 4. Average far-UV lineshapes and multicomponent fits.

Figure 4 illustrates an example of what one can do with the broad consistent UV coverage by STIS: it shows a decomposition of an average UV hot-line profile (light [yellow] shaded) from the active G giant μ Vel, obtained by scaling and coadding all the components of the Si IV, C IV, and N V doublets. The smaller darker (green) shaded profile is an average of chromospheric O I and C I lines, for comparison. For most stars, the hot-line profiles are nearly identical in shape, aside from a few instances of weak blends (which are suppressed in the coaddition procedure); so the average profile provides enhanced information on the mean dynamical properties of the outer atmosphere. Note the extended blue wing on the average hot-line profile of μ Vel. This behavior is not seen in any of the other active giants analyzed in this way, and undoubtedly reflects transient flare activity during the several STIS orbits devoted to the E140M exposure.

Table 1 summarizes properties of the decomposed average hot-line profiles of four separate groups of stars. The average standard deviations within each sample are as follows: column #3, $\sim$ 1 km s^{-1}; column #4, $\sim$ 5 km s^{-1}; column #5, $\sim$ 4 km s^{-1}; column #6, 3–30 km s^{-1}. Note that the narrow components are dominantly *redshifted* in all the stars, yet the velocity amplitude decreases with increasing surface gravity (G→M, III→V). The broad components also are dominantly redshifted, with an amplitude typically *twice* that of the corresponding narrow component. The broad component flux ranges from about 20% up to 60% of the total, well correlated with the $R_{\rm CIV}$ activity index. Finally, in both the dwarfs and giants, the broad components are about 2.7× wider than the narrow components, while the narrow components of the giants are about 1.6× wider than the narrow components of the dwarfs. Measurements like these will provide important input into future discussions of coronal heating mechanisms; a key legacy of STIS for the cool-star UV community.

Table 1. Broad and Narrow Components.

Group	$N_\star$	$v_{\rm narrow}$	$W_{\rm n}$	$v_{\rm broad}$	$W_{\rm b}$	$f_{\rm b}/f_{\rm tot}$
(1)	(2)	(3)	(4)	(5)	(6)	(7)
G V	5	+4.3	43	+5.9	103	0.22–0.54
K V	3	+2.2	32	+6.8	78	0.46–0.56
M V	4	+1.6	32	+8.0	105	0.35–0.42
G III	4	+6.5	59	+12.2	156	0.49–0.61

Notes: W is FWHM, v is Doppler shift; both in km s^{-1}

Acknowledgements

This work was supported by grants HST–AR–09550.01 from STScI and NAG5–13058 from NASA. Observations from the NASA/ESA *HST,* were collected at the STScI, operated by AURA, under contract NAS5-26555.

References

Ayres, T. R., et al. 2003, ApJ, 583, 963
Ayres, T. R., et al. 2001, ApJ, 549, 554
Pagano, I., et al. 2004, A&A, 415, 331
Redfield, S., Wood, B. E., & Linsky, J. L. 2004, AdSpR, 34, 41
Wood, B. E. 2004, LRSP, 1, 2
Wood, B. E., Linsky, J. L., & Ayres, T. R. 1997, ApJ, 478, 745
Woodgate, B. E., et al. 1998, PASP, 110, 1183